ELSEVIER

$Bi_{2/3}Ce_{1/3}Rh_2O_5$: A new mixed-valent Rh oxide with hitherto unknown structure

Hiroshi Mizoguchi[a], A.P. Ramirez[b], L.N. Zakharov[a], A.W. Sleight[a], M.A. Subramanian[a],*

[a]Department of Chemistry, and OSUMI, Oregon State University, Corvallis, OR 97331-4003, USA
[b]Bell Laboratories, Alcatel-Lucent, 600 Mountain Avenue, Murray Hill, NJ 07974, USA

Abstract

The new compound $Bi_{2/3}Ce_{1/3}Rh_2O_5$ has been discovered. It is currently the only known compound in the Bi–Ce–Rh–O system, and it crystallizes in a previously unknown structure type. The structure was established from single crystal X-ray diffraction data. Interatomic distances indicate the oxidation states as $Bi^{3+}_{2/3}Ce^{4+}_{1/3}Rh^{3.33+}_2O_5$. The structure indicates no ordering between Rh^{3+} and Rh^{4+}. The lack of charge ordering is consistent with the metallic properties determined from electrical conductivity, Seebeck coefficient, and magnetic susceptibility measurements.
© 2007 Elsevier Inc. All rights reserved.

Keywords: Mixed valency; Crystal structure; Electrical conductivity; Seebeck coefficient; Magnetic properties

1. Introduction

Rhodium is commonly found as Rh^{3+} or Rh^{4+} in oxides. Synthesis in air usually gives Rh^{3+} oxides. The synthesis of Rh^{4+} oxides normally needs a larger partial pressure of oxygen [1–4]. However, the existence of electropositive countercations such as Ba^{2+} often enhances the formation of Rh^{4+} even for synthesis under air [5–11].

Several interesting compounds have been found in the Bi–Rh–O system. Pyrochlore-type $Bi_2Rh_2O_{6.8}$ is synthesized easily under air, although it does not contain electropositive cations [12]. It is considered as having 0.8 positive holes per formula unit in a valence band composed of Rh 4d–O 2p t^*_{2g}, and in fact, a high electrical conductivity of 330 S/cm at 300 K is reported. Another mixed-valent Rh compound, $(Bi_6O_5)Rh_{12}O_{24}$, reported very recently has the Todolokite structure [13,14]. This structure is related to the rutile and Hollandite structures and has large channels containing Bi_6O_5 chains. In $(Bi_6O_5)Rh_{12}O_{24}$ there is evidence for charge ordering, consistent with its semiconducting behavior. The perovskite-type structure is found for $BiRhO_3$, which is prepared at high pressure [12]. Apparently, the only compound known in the Ce–Rh–O system is $CeRhO_3$ with a perovskite-type structure [15].

Our investigations of the Bi–Ce–Rh–O system revealed the existence of the new compound, $Bi_{2/3}Ce_{1/3}Rh_2O_5$, which occurs in a structure apparently not previously observed.

2. Experimental

Reactants were Bi_2O_3 (99.9%, Baker), CeO_2 nanopowder (99.9%, Aldrich), V_2O_5 (99.9%, Johnson Matthey) and Rh_2O_3 prepared from $RhCl_3 \times H_2O$ (99.9%, Alfa, Aesar) by heating in moist air at 1073 K for 10 h. Appropriate amounts of Bi_2O_3, CeO_2, and Rh_2O_3 were mixed by grinding together under ethanol in an agate mortar. This pressed mixture was placed in an alumina boat and heated in air at 1073, 1173, and 1273 K each for 10 h with intermediate grindings. Single crystals of $Bi_{2/3}Ce_{1/3}Rh_2O_5$ were grown in a flux of 90 wt% Bi_2O_3 and 10 wt% V_2O_5. An intimate mixture of polycrystalline CeO_2 (0.18 g), Rh_2O_3 powder (0.14 g), Bi_2O_3 (3.5 g), V_2O_5 (0.38 g) was heated to 1373 K under air in a covered alumina crucible. After holding for 10 h, the crucible was cooled to 973 K at a

*Corresponding author. Fax: +1 541 737 2062.
E-mail address: mas.subramanian@oregonstate.edu
(M.A. Subramanian).

rate of 3 K/h. After reaching 973 K, it was cooled to room temperature at a rate of 300 K/h. The flux was dissolved in HNO_3(aq) at 360 K. The product consisted of lustrous black crystals with several hundred micrometers in length. Attempts to substitute La, Nd, Y for Bi or Zr, Hf, Pr, or Tb for Ce failed.

The cationic composition was determined by a CAMECA SX100 electron microprobe analyzer. No vanadium or aluminum could be detected in the crystals. Single crystal X-ray diffraction data were collected on a Bruker SMART APEXII CCD system at 173 K. A standard focus tube was used with an anode power of 50 kV at 30 mA, a crystal to plate distance of 5.0 cm, 512×512 pixels/frame, beam center (256.52, 253.16), total frames of 6602, oscillation/ frame of 0.50°, exposure/frame of 10.0 s/frame and SAINT integration. A subsequent SADABS correction was applied. The crystal structure was solved with the direct method program SHELXS and refined with full-matrix least-squares program SHELXTL [16]. Further details are given in Tables 1 and 2, and in available cif files.

DC electrical conductivity measurements were conducted by conventional four probe methods over the temperature region 80–300 K. Seebeck coefficient measurements were conducted over the temperature region 120–300 K. Magnetic measurements were made using a Quantum Design Magnetic Property Measurement System. EUTAX software was used to calculate bond valences [17].

Table 1
Crystal data and structure refinement for $Bi_{2/3}Ce_{1/3}Rh_2O_5$

Empirical formula	$Bi_{0.67}Ce_{0.33}O_5Rh_2$
Formula weight	471.03
Temperature	173(2) K
Wavelength	0.71073 Å
Crystal system	Orthorhombic
Space group	$Pnma$
Unit cell dimensions	$a = 7.1298(9)$ Å, $\alpha = 90°$
	$b = 9.9666(12)$ Å, $\beta = 90°$
	$c = 5.1067(6)$ Å, $\gamma = 90°$
Volume	362.88(8) Å³
Z	4
Density (calculated)	8.622 g/cc
Absorption coefficient	45.119 mm⁻¹
$F(000)$	817
Crystal size	$0.05 \times 0.04 \times 0.03$ mm³
Theta range for data collection	4.09–27.48°
Index ranges	$-9 \leqslant h \leqslant 9$, $-12 \leqslant k \leqslant 12$, $-6 \leqslant l \leqslant 6$
Reflections collected	3703
Independent reflections	442 [R(int) = 0.0234]
Completeness to $\theta = 27.48°$	99.5%
Absorption correction	Semi-empirical from equivalents
Max. and min. transmission	0.3447 and 0.2113
Refinement method	Full-matrix least-squares on F^2
Data/restraints/parameters	442/1/43
Goodness-of-fit on F^2	1.212
Final R indices [$I > 2\sigma(I)$]	$R_1 = 0.0217$, w$R_2 = 0.0508$
R indices (all data)	$R_1 = 0.0230$, w$R_2 = 0.0513$
Extinction coefficient	0.0041(3)
Largest diff. peak and hole	2.043 and −2.123 e Å⁻³

Table 2
Atomic coordinates and displacement factors for $Bi_{2/3}Ce_{1/3}Rh_2O_5$

	Wyckoff	x	y	z	U(eq) (Å $\times 10^3$)[a]
(Ce,Bi)	4c	0.7386(1)	0.75	0.2154(1)	6(1)
Rh	8d	0.5798(1)	0.4410(1)	0.2498(1)	4(1)
O1	8d	0.3318(7)	0.4493(5)	0.065(1)	7(1)
O2	4c	0.620(1)	0.25	0.0951(15)	10(2)
O3	8d	0.4805(7)	0.3801(5)	0.597(1)	6(1)

[a] U(eq) is defined as one-third of the trace of the orthogonalized U^{ij} tensor.

3. Results

The structure of $Bi_{2/3}Ce_{1/3}Rh_2O_5$ is shown in Fig. 1, and some bond distances and angles are given in Table 3. The ratio of Bi-to-Ce on the 4c site was confirmed by both chemical analysis and refinement of occupation factors. A notable feature is the zigzag chains of edge-shared Rh octahedra extending along the c-axis. The same type of chains exists in other structures such as the α-PbO_2 structure (Fig. 1) [18]. A difference between the $Bi_{2/3}Ce_{1/3}Rh_2O_5$ and α-PbO_2 structures is the way the chains are connected to each other. The O atoms joining the chains in α-PbO_2 all have a coordination number of three. In the case of $Bi_{2/3}Ce_{1/3}Rh_2O_5$ some of the O atoms joining the chains have a coordination number of two.

A similarity of the $Bi_{2/3}Ce_{1/3}Rh_2O_5$ structure to the structures of $BaNb_2O_6$ and $BaTi_4O_9$ is shown in Fig. 2 [19–21]. For all three structures, networks of linked octahedra form similar channels for the A cations Ba, Bi, and Ce. The polyhedra around these A cations is shown in Fig. 2. Perpendicular to these channels the A cations form a hexagonal array, although the actual symmetry is orthorhombic in all cases. The way that the octahedra are linked is, however, much different in these three structures. There are no edge-shared chains in $BaNb_2O_6$. Instead, there are octahedra sharing edges in pairs, which are then linked by corners to form chains along the a-axis. In $BaTi_4O_9$ there are edge-shared chains along the b-axis, but with much more edge sharing than in $Bi_{2/3}Ce_{1/3}Rh_2O_5$. In $Bi_{2/3}Ce_{1/3}Rh_2O_5$ each octahedron shares just two edges to form the zigzag chains. There are two such zigzag chains in $BaTi_4O_9$, which share edges with each other so that each octahedron shares six of its 12 edges with other octahedra.

Fig. 3 shows the electrical conductivity of a $Bi_{2/3}Ce_{1/3}Rh_2O_5$ pellet from 80 to 300 K. The temperature dependence is metal like with a conductivity of 60 S/cm at 300 K. This is a low value for a metal but is typical for Rh oxides showing such temperature dependence [4,22,23]. As shown in the inset, the behavior obeys the equation: $\rho = \rho_0 + AT^2$, indicative of a Fermi liquid. The fitting gives $A = 0.0734$ ($10^{-6}\,\Omega\,cm\,K^{-2}$). Fig. 3 also shows the temperature dependence of Seebeck coefficients. The small values of $\sim$4–5 μV/K are consistent with the metallic temperature dependence of the electrical conductivity. Fig. 4 shows the
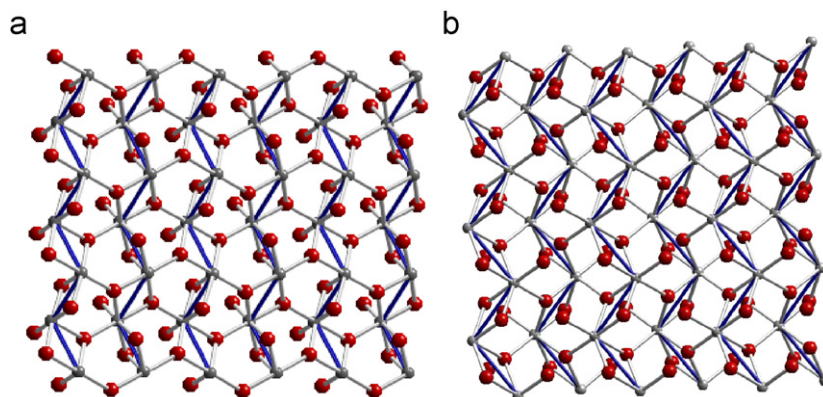
Fig. 1. Zigzag chains emphasized using "bonds" between the metal atoms sharing the octahedral edges in (a) $Bi_{2/3}Ce_{1/3}Rh_2O_5$ and (b) α-PbO_2. The light grey atoms are Rh or Pb and are surrounded by oxygen atoms (red in online version) which form octahedral network.

Table 3
Structural features for $Bi_{2/3}Ce_{1/3}Rh_2O_5$

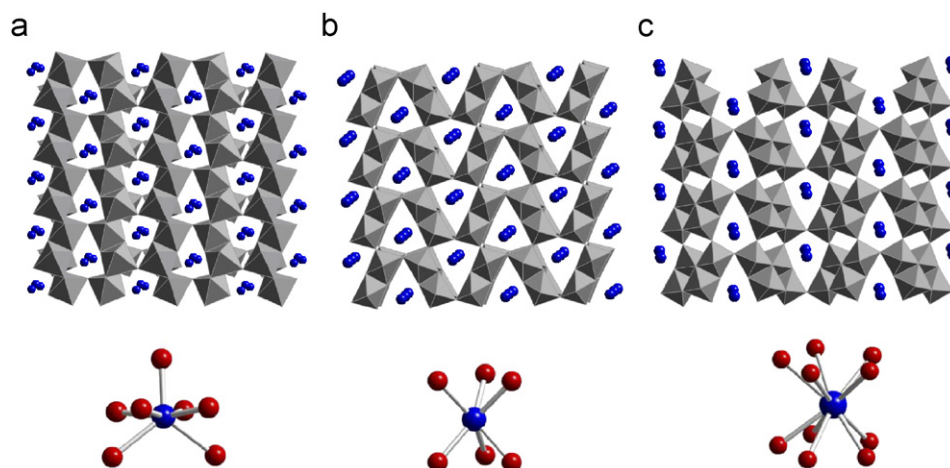| Rh–O distances (Å)	Bi/Ce–O distances (Å)	Rh–O–Rh angles (deg)	Rh–Rh distances (Å)
O(1) 2.004(5) 2.031(5)	O(1) 2.501(5)*2	O(1) 96.9(2)	3.031(1) 3.034(1)
O(2) 2.046(5) 2.081(3)	O(2) 2.186(7)		
O(3) 1.993(5) 2.005(5)	O(3) 2.244(5)*2 2.461(5)*2	O(3) 98.7(2)	

Fig. 2. Crystal structure projections of: (a) $Bi_{2/3}Ce_{1/3}Rh_2O_5$, (b) $BaNb_2O_6$ and (c) $BaTi_4O_9$ with polyhedra of A cations underneath. The projection shows octahedral network formed by Rh, Nb and Ti respectively. Underneath, the dark grey atoms (dark blue in online version) are Bi, Ce or Ba and the light grey atoms are oxygen (red in online version).

temperature dependence of magnetic susceptibility per Rh ion. The data were fitted with the equation $\chi = \chi_0 + C/(T-\theta)$ to give a χ_0 value of 1.5×10^{-4} emu mol^{-1}, $C = 2.93 \times 10^{-3}$ emu mol^{-1} K^{-1}, and $\theta = 0.52$ K. Thus, the steep increase near 20 K is likely due to a paramagnetic impurity. Assuming ρ_0 is a Fermi liquid term, it's value implies a specific heat linear term with a prefactor ($= 11$ mJ/mole Rh K^2). The magnitude of this term is similar to that found in other Rh-based metals and also consistent with the Seebeck coefficient.

4. Discussion

The possible oxidation states to consider in $Bi_{2/3}Ce_{1/3}$ Rh_2O_5 for both Rh and Ce are $+3$ and $+4$. Assuming that Bi is Bi^{3+}, the average oxidation state for Rh must be
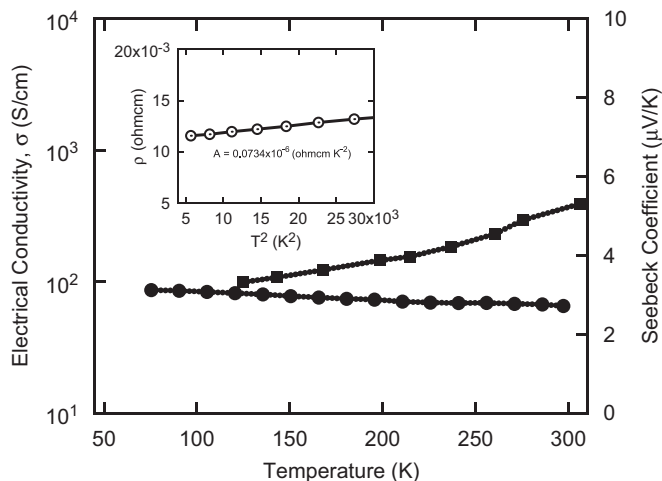
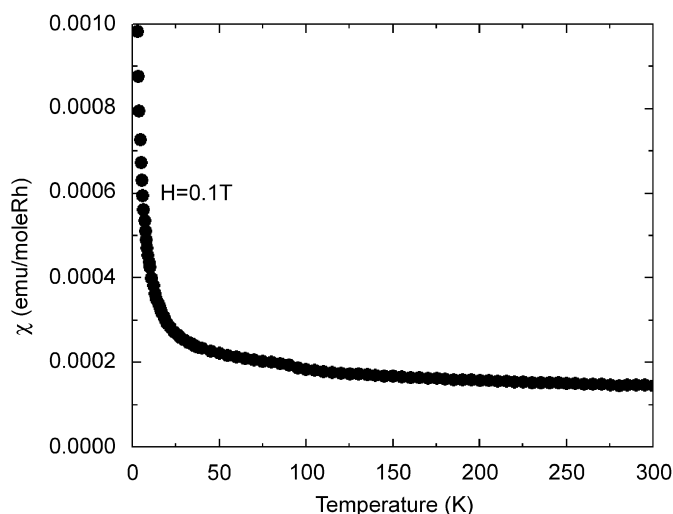Fig. 3. Electrical conductivity (●) and Seebeck coefficient (■) of $Bi_{2/3}Ce_{1/3}Rh_2O_5$ vs. temperature.

Fig. 4. Magnetic susceptibility of $Bi_{2/3}Ce_{1/3}Rh_2O_5$ vs. temperature.

between $+3$ and $+4$. Given the fact the binary oxides stable in air are CeO_2 and Rh_2O_3, it might be concluded that the Ce is Ce^{4+}. It is, however, not entirely safe to make such an assumption for a ternary oxide. Therefore, we consider the possibility that Ce could be either Ce^{3+} or Ce^{4+}. Thus, $Bi_{2/3}Ce_{1/3}Rh_2O_5$ might be either $Bi_{2/3}Ce_{1/3}^{4+}Rh_2^{3.33+}O_5$ or $Bi_{2/3}Ce_{1/3}^{3+}Rh_2^{3.5+}O_5$. In either case Rh would be mixed valent. Bond valence calculations give a bond valence of 3.18 for Rh, suggesting that the valence of Rh in $Bi_{2/3}Ce_{1/3}Rh_2O_5$ is more likely 3.33 than 3.5. Bond valence calculations are not possible for a site occupied by two different elements. However, use of the weighted ionic radii for Bi and Ce gives a predicted (Bi,Ce)–O bond distance of 2.46 Å assuming Ce^{3+} and 2.41 Å assuming Ce^{4+}. Given that the observed average of this distance is 2.37 Å, we would again conclude that Ce is Ce^{4+}.

The mixed valency Rh suggests that the ratio of Bi-to-Ce should be variable. However, our attempts to vary this ratio always led to products with second phases present and no discernible change in the cell dimensions of the $(Bi,Ce)Rh_2O_5$ phase. This invariance suggests that there is one-dimensional ordering of Bi and Ce along the a-axis. The metal–metal distance along this direction is 3.58 Å, and the ordering would be –Ce–Bi–Bi–Ce–Bi–Bi–. The (Bi,Ce) atoms form a hexagonal array perpendicular to the a-axis (Fig. 2(a)) with four metal–metal distances of 5.60 Å and two of 5.11 Å. These much longer distances could preclude three-dimensional ordering of Bi and Ce.

Many rhodium oxides are known with Rh^{3+}/Rh^{4+} mixed valency [5–10,12–14,22–25]. The only two cases where evidence has been presented for charge ordering are $(Bi_6O_5)Rh_{12}O_{24}$ and $Ln_{18}Li_8Rh_5O_{39}$ where Ln can be La or Pr [14,24]. The structure and properties of $Bi_{2/3}Ce_{1/3}Rh_2O_5$ indicate that no charge ordering occurs. It could be that the disorder of Bi and Ce has prevented such order.

Acknowledgments

Appendix A. Supplementary materials

Crystallographic data associated with this article can be obtained from the Fachinformationzentrum Karlsruhe, D-76344 Eggenstein-Leopoldshafen, Germany (E-mail: Crysdata@fiz-karlsruhe.de) on quoting depository number: 418646.

References

[1] R.D. Shannon, Solid State Commun. 6 (1968) 139–143.
[2] O. Muller, R. Roy, J. Less-Common Met. 16 (1968) 129–146.
[3] A.W. Sleight, J.L. Gilson, Mater. Res. Bull. 6 (1971) 781–784.
[4] K. Yamaura, E. Takayama-Muromachi, Phys. Rev. B 64 (2001) 224424.
[5] T. Siegrist, E.M. Larson, B.L. Chamberland, J. Alloys Compd. 210 (1994) 13–17.
[6] J.B. Claridge, H.-C. zur Loye, Chem. Mater. 10 (1998) 2320–2322.
[7] J.R. Plaisier, A.A.C. van Vliet, D.J.W. Ijdo, J. Alloys Compd. 314 (2001) 56–61.
[8] K.E. Stitzer, M.D. Smith, J. Darriet, H.-C. zur Loye, Chem. Commun. (2001) 1680–1681.
[9] K.E. Stitzer, E.A. Abed, J. Darriet, H.-C. zur Loye, J. Amer. Chem. Soc. 126 (2004) 856–864.
[10] T. Klimczuk, W.-L. Lee, H.W. Zandbergen, R.J. Cava, Mater. Res. Bull. 39 (2004) 1671–1677.
[11] T. Shimura, M. Itoh, T. Nakamura, J. Solid State Chem. 98 (1992) 198–200.
[12] J.M. Longo, P.M. Raccah, J.A. Kafalas, J.W. Pierce, Mater. Res. Bull. 7 (1972) 137–146.
[13] F. Stowasser, C. Renkenberger, Z. Kristallogr. 221 (2006) 206–212.
[14] H. Mizoguchi, W.J. Marshall, A.P. Ramirez, A.W. Sleight, M.A. Subramanian, J. Solid State Chem., 2007, doi:10.1016/j.jssc/2007.09.031.

[15] V.B. Lazarev, I.S. Shaplygin, Russ. J. Inorg. Chem. 23 (1978) 2614–2621.
[16] G.M. Sheldrick, SHELEXTL, Version 6.14, Bruker Analytical X-ray Instruments, Inc., Madison, WI, 2003.
[17] N.E. Brese, M. O'Keeffe, Acta Crystallogr. B 47 (1991) 192–197.
[18] A.I. Zaslavskii, Y.D. Kondrashev, S.S. Talkachev, Dokl. Akad. Nauk SSSR 75 (1950) 559–561.
[19] F. Gallaso, G. Layden, G. Ganung, Mater. Res. Bull. 3 (1968) 397–408.
[20] V.P. Sirotinkin, S.P. Sirotinkin, Russ. J. Inorg. Chem. 35 (1990) 1246–1248.
[21] W. Hofmeister, E. Tillmanns, W.H. Baur, Acta Crystallogr. C 40 (1984) 1510–1512.
[22] T. Nakamura, T. Shimura, M. Ito, Y. Takeda, Solid State Chem. 103 (1993) 523–527.
[23] K. Yamaura, Q. Huang, M. Moldovan, D.P. Young, A. Sato, Y. Baba, T. Nagai, Y. Matsui, E. Takayama-Muromachi, Chem. Mater. 17 (2005) 359–365.
[24] P.P.C. Frampton, P.D. Battle, C. Ritter, Inorg. Chem. 44 (2005) 7138–7142.
[25] H.S. Jarrett, A.W. Sleight, H.H. Kung, J.L. Gilson, J. Appl. Phys. 51 (1980) 3916–3925.